

Fresnel zones in tapered gradient-index media

José Manuel Rivas-Moscoso, Carlos Gómez-Reino, and María Victoria Pérez

Laboratorio de Óptica, Departamento de Física Aplicada, Facultad de Física and Escola de Óptica e Optometría, Universidade de Santiago de Compostela, Campus Sur, E15782 Santiago de Compostela, Spain

Received April 8, 2002; revised manuscript received June 13, 2002; accepted June 18, 2002

The free propagation of a wave front in an inhomogeneous medium with parabolic refractive-index profile and the division of the wave front into Fresnel zones are studied. We determine the radius and the area of each zone as well as the zone contribution to the total wave at an observation point inside the medium. We find the condition that the optical path must fulfill from each zone to that point so that the disturbance due to successive zones will be in phase opposition. Once this condition is settled the concept of zone plate in gradient-index media is introduced. © 2002 Optical Society of America
 OCIS codes: 110.2760, 350.5500.

1. INTRODUCTION

Fresnel zones resulting from the division of a wave front that propagates in a homogeneous medium are well known in optics and have received widespread attention. Fundamental properties and many practical applications have been considered.¹ Fresnel zones and zone plates have played and still play a leading role in the study of propagation and diffraction of light through homogeneous media. Recently Rivas-Moscoso *et al.* studied light propagation through hybrid optical structures formed by a zone plate located at the input plane of a tapered gradient-index (GRIN) medium and the influence of off-axis illumination and finite dimension on light propagation.^{2,3} The purpose of the present paper is to generalize the zone division of a wave front for light propagation in GRIN media and to discuss the imaging properties of zone plates in these media as a logical continuation of the previous papers. We have found information on this topic only in Ref. 4, where the shape of the first Fresnel zone is obtained by making use of the method of stationary phase in the geometrical-optics approximation.

The plan of the paper is as follows. In Section 2 we obtain the general expression for the complex-amplitude distribution at a point within an inhomogeneous medium after free propagation of a wave front in it. In Section 3 we divide this wave front into zones and calculate the radii and areas of those zones. In Section 4 we study the irradiance distribution along the optical axis to see where the maxima and minima of irradiance occur. In Section 5 we obtain the contribution of each zone to the total disturbance at an observation point as well as the addition of the contributions of an odd and even number of zones. In Section 6 we deal with the zone-plate construction in GRIN media and establish an analogy with the lens imaging formula, and we apply the results to various types of taper functions. Finally, in Section 7 we present our conclusions.

2. FREE PROPAGATION OF A WAVE FRONT IN GRADIENT-INDEX MEDIA: GENERAL EXPRESSION

Let us consider a tapered GRIN medium characterized by a transverse parabolic refractive index modulated by an axial index and whose refractive-index profile is given by

$$n^2(x, z) = n_0^2[1 - g^2(z)r^2]; \quad r^2 = x^2 + y^2, \quad (1)$$

where n_0 is the index at the z optical axis and $g(z)$ is the taper function that describes the evolution of the transverse parabolic index distribution along the z axis.

A point source within the medium emits light that propagates a distance z , producing a disturbance at a point (r_0, z) that can be expressed, in parabolic approximation, by the following wave front,

$$\psi(r_0; z) = \frac{kn_0}{2\pi i H_1(z)} \exp(ikn_0z) \times \exp\left\{i \frac{kn_0}{2H_1(z)} [r_0^2 \dot{H}_1(z)]\right\}, \quad (2)$$

where $H_1(z)$ and $\dot{H}_1(z)$ are the position and the slope of the axial ray and the dot represents the derivative with respect to z .⁵ From Eq. (2) it follows that the curvature radius of the wave front can be written as

$$R(z) = \frac{H_1(z)}{n_0 \dot{H}_1(z)}. \quad (3)$$

The complex-amplitude distribution at a point (r, z') inside the medium (see Fig. 1) can be calculated from the wave front Σ in Eq. (2) by solving the diffraction integral⁵

$$\psi(r; z') = \int_{\Sigma} K(r, r_0; z') \psi(r_0; z) d\Sigma, \quad (4)$$

where $K(r, r_0; z')$ is the kernel or propagator for GRIN media in cylindrical coordinates,

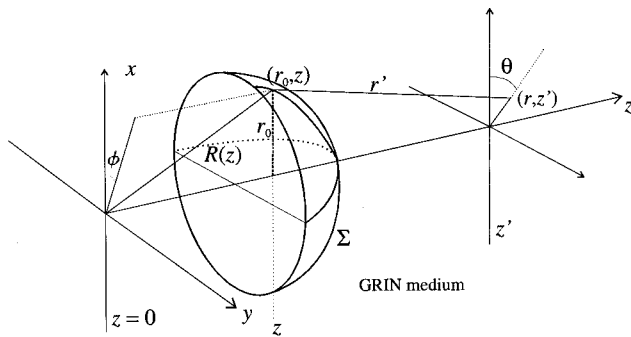


Fig. 1. Geometry for the propagation and division of a wave front in a GRIN medium

$$K(r, r_0; z') = \frac{-ikn_0}{2\pi H_1(z')} \exp[ikn_0(z' - z)] \\ \times \exp\left\{ \frac{ikn_0}{2H_1(z')} [H_1(z')r^2 + H_2(z')r_0^2 - 2rr_0 \cos(\phi - \theta)] \right\}, \quad (5)$$

$d\Sigma$ is the surface element, which can be expressed as

$$d\Sigma = \left[1 + \frac{\dot{H}_1^2(z)}{H_1^2(z)} r_0^2 \right]^{1/2} r_0 dr_0 d\phi, \quad (6)$$

and $H_1(z')$, $H_2(z')$, $\dot{H}_1(z')$, and $\dot{H}_2(z')$ are, respectively, the position and the slope of the axial and field rays at z' after propagating from z . This involves changing the integration limits in the argument of the sine and cosine functions in the expressions of $H_1(z)$, $H_2(z)$ and $\dot{H}_1(z)$, $\dot{H}_2(z)$ given in Ref. 5, which now go from z to z' .

Substitution of Eqs. (2), (5), and (6) into Eq. (4) provides

$$\psi(r; z') = -\frac{k^2 n_0^2 \exp(ikn_0 z')}{2\pi H_1(z')} \exp\left[i \frac{kn_0}{2H_1(z')} \dot{H}_1(z') r^2 \right] \\ \times \int \frac{1}{H_1(z)} J_0 \left[\frac{kn_0 r r_0}{H_1(z)} \right] \\ \times \exp\left\{ i \frac{kn_0}{2} \left[\frac{\dot{H}_1(z)}{H_1(z)} + \frac{H_2(z')}{H_1(z')} \right] r_0^2 \right\} \\ \times \left[1 + \frac{\dot{H}_1^2(z)}{H_1^2(z)} r_0^2 \right]^{1/2} r_0 dr_0, \quad (7)$$

where J_0 is the zero-order Bessel function of the first kind. This is the general expression for the complex amplitude distribution at a point (r, z') after propagation of a wave front Σ in the parabolic approximation.

3. WAVE-FRONT DIVISION: ZONE RADII AND AREAS

Following Fresnel, instead of directly solving the integral in Eq. (6), we divide the wave front Σ into zones. For that purpose we consider a circular aperture with radius h and assume slow variations of z within the zone deter-

mined by this aperture. Furthermore, we restrict the study to observation points on the optical axis and to wave fronts sufficiently far from the image planes, where $H_1(z) = 0$. This allows us to develop the surface element in power series up to second order and to avoid the singularity that exists at those planes. With these conditions kept in mind, Eq. (7) becomes

$$\psi(z') = \zeta(z, z') \int_0^h \exp\left[i \frac{B(z, z')}{2} r_0^2 \right] \\ \times \left[1 + \frac{1}{2} \frac{\dot{H}_1^2(z)}{H_1^2(z)} r_0^2 \right] r_0 dr_0, \quad (8)$$

whose solution is

$$\psi(z') = \frac{\zeta(z, z')}{iB(z, z')} \left[\left\{ \exp\left[i \frac{B(z, z')}{2} h^2 \right] - 1 \right\} \right. \\ \left. + \frac{\dot{H}_1^2(z)}{2H_1^2(z)} \left(h^2 \exp\left[i \frac{B(z, z')}{2} h^2 \right] - \frac{2}{iB(z, z')} \right) \right. \\ \left. \times \left\{ \exp\left[i \frac{B(z, z')}{2} h^2 \right] - 1 \right\} \right] \quad (9)$$

and where we have defined

$$\zeta(z, z') = -\frac{k^2 n_0^2}{2\pi H_1(z') H_1(z)} \exp(ikn_0 z') \\ \times \exp\left[i \frac{kn_0}{2H_1(z')} \dot{H}_1(z') r^2 \right] \quad (10)$$

$$B(z, z') = kn_0 \left[\frac{\dot{H}_1(z)}{H_1(z)} + \frac{H_2(z')}{H_1(z')} \right]. \quad (11)$$

The corresponding irradiance can be written as

$$I(z') = \frac{k^2 n_0^2}{\pi^2 [\dot{H}_1(z) H_1(z') + H_2(z') H_1(z)]^2} \\ \times \sin^2 \left[\frac{B(z, z')}{4} h^2 \right] \left[1 + \frac{h^2 \dot{H}_1^2(z)}{2H_1^2(z)} \right] \quad (12)$$

after we disregard the terms that go with $\dot{H}_1^4(z)/H_1^4(z)$ since their contribution under the imposed restriction that the wave front must be sufficiently far from the image planes—or, equivalently, $\dot{H}_1(z) \ll H_1(z)$ —is negligible.

The radius h assumes certain values for which maxima and minima of irradiance are reached at a point z' . Those values can be evaluated by differentiating Eq. (12) with respect to h and making the result equal to zero:

$$2B(z, z') \left[1 + \frac{h^2 \dot{H}_1^2(z)}{2H_1^2(z)} \right] \sin \left[\frac{B(z, z')}{2} h^2 \right] = 0. \quad (13)$$

This equation is fulfilled by the values h_j resulting from

$$\begin{aligned}
 h_j^2 &= \frac{j\lambda H_1(z)H_1(z')}{n_0[H_2(z')H_1(z) + H_1(z')\dot{H}_1(z)]} \\
 &= \frac{j\lambda H_1(z')R(z)}{n_0 H_2(z')R(z) + H_1(z')}, \quad (14)
 \end{aligned}$$

where j is an integer that assumes an even value for minima and an odd value for maxima and where Eq. (3) has been used. In Fig. 2 we represent the irradiance I as a function of the radius h and its square. Equation (14) predicts the positions of maxima and minima as well as the periodicity of the irradiance with h^2 . Making use of this result, we proceed to the division of the wave front Σ into zones whose radii are given by Eq. (14). Radii h_j permit definition of the distance r_j from z' to the upper end of the j th zone (see Fig. 3) as

$$\begin{aligned}
 r_j &= (z' - z) \\
 &+ \frac{j\lambda H_1(z')H_1(z)}{2(z' - z)n_0[H_2(z')H_1(z) + \dot{H}_1(z)H_1(z')]} \\
 &= (z' - z) + \frac{j\lambda H_1(z')R(z)}{2(z' - z)[n_0 H_2(z')R(z) + H_1(z')]}, \quad (15)
 \end{aligned}$$

which has been developed in power series up to second order.

In contrast, the distance s_j between the plane containing the j th zone and the vertex of the wave front can be easily calculated by using Eqs. (14) and (15) to give

$$\begin{aligned}
 s_j &= \frac{j\lambda \dot{H}_1(z)H_1(z')}{2n_0[\dot{H}_1(z)H_1(z') + H_1(z)H_2(z')]} \\
 &= \frac{j\lambda H_1(z')}{2n_0[H_1(z') + n_0 R(z)H_2(z')]}, \quad (16)
 \end{aligned}$$

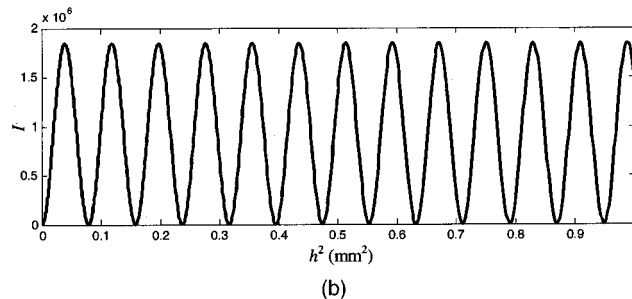
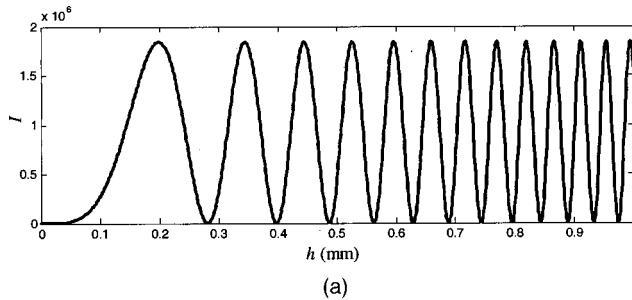


Fig. 2. Irradiance I in a GRIN medium with $n_0 = 1.5$ and $g_0 = 0.1 \text{ mm}^{-1}$ as a function of (a) the radius h and (b) the square of h .

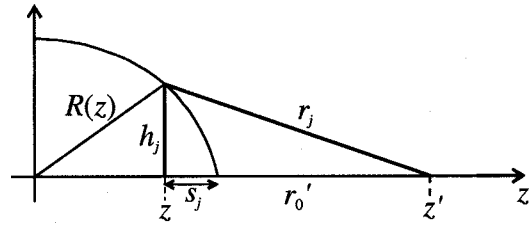


Fig. 3. Parameters for the division of the wave front into zones. By integration of the surface element $d\Sigma$ within the limits of each zone, we can determine the zone areas, which are given by

$$\begin{aligned}
 \Sigma_j &= \int_{h_j}^{h_{j+1}} d\Sigma_j = \frac{\pi\lambda H_1(z')H_1(z)}{n_0[H_2(z')H_1(z) + H_1(z')\dot{H}_1(z)]} \\
 &= \frac{\pi\lambda H_1(z')R(z)}{n_0 H_2(z')R(z) + H_1(z')}. \quad (17)
 \end{aligned}$$

Note that there is no dependence on j and that the zone areas are very nearly equal.

At the Fourier transform planes [$\dot{H}_1(z) = 0$] the wave-front curvature becomes zero [$1/R(z) \rightarrow 0$], and consequently there are no variations of z within a zone. This fact allows the simplification of Eqs. (9)–(17), the irradiance at a point z' being

$$I_{\text{FT}}(z') = \frac{k^2 n_0^2}{\pi^2 H_1^2(z)H_2^2(z')} \sin^2 \left[\frac{B(z, z')}{4} h^2 \right], \quad (18)$$

the distance

$$r_j = (z' - z) + \frac{j\lambda H_1(z')}{2n_0 H_2(z')(z' - z)}, \quad (19)$$

and the expressions of the zone radii and areas

$$h_j^2 = \frac{j\lambda H_1(z')}{n_0 H_2(z')}, \quad (20)$$

$$\Sigma_j = \frac{\pi\lambda H_1(z')}{n_0 H_2(z')}, \quad (21)$$

respectively. In both the general case [Eqs. (9)–(17)] and the particular case in which we restrict ourselves to wave fronts at the Fourier transform planes [Eqs. (18)–(21)], all the expressions duplicate the classic results for homogeneous media⁶ by making $H_1(z') \rightarrow z' - z$ and $H_2(z') \rightarrow 1$.

4. IRRADIANCE DISTRIBUTION ALONG THE OPTICAL AXIS

In Section 3 the zone radii that produced maxima and minima of irradiance for a certain observation plane z' were determined. Now we set a value for the aperture radius h and see how the irradiance evolves through the GRIN medium. We consider two cases to evaluate the maxima and minima positions: wave front at Fourier transform planes and wave front off Fourier transform planes.

A. Wave Front at Fourier Transform Planes

Maxima and minima positions can be obtained by differentiating the irradiance given by Eq. (18) with respect to z' and making it equal to zero. To gain clarity, we will

apply the equation to a selfoc medium, that is, a medium in which $g(z)$ is a constant. For this medium the axial and the field rays are given, respectively, by⁵

$$H_1(z) = g_0^{-1} \sin(g_0 z),$$

$$H_1(z') = g_0^{-1} \sin[g_0(z' - z)] \quad (22)$$

and

$$H_2(z) = \cos(g_0 z), \quad H_2(z') = \cos[g_0(z' - z)], \quad (23)$$

where g_0 is the gradient parameter.

The derivative equalized to zero becomes

$$\frac{\sin^2\left\{\frac{kn_0}{4} \frac{h^2 g_0}{\tan[g_0(z' - z)]}\right\}}{\cos[g_0(z' - z)]} - \frac{kn_0}{4} h^2 g_0$$

$$\times \frac{\sin\left\{\frac{kn_0}{4} \frac{h^2 g_0}{\tan[g_0(z' - z)]}\right\} \cos\left\{\frac{kn_0}{4} \frac{h^2 g_0}{\tan[g_0(z' - z)]}\right\}}{\sin^3[g_0(z' - z)]} = 0. \quad (24)$$

Minima will be at positions satisfying

$$\sin\left\{\frac{kn_0}{4} \frac{h^2 g_0}{\tan[g_0(z' - z)]}\right\} = 0, \quad (25)$$

which correspond to

$$z'_{\min} = \frac{1}{g_0} \tan^{-1}\left(\frac{n_0 h^2 g_0}{2m\lambda}\right) + z, \quad (26)$$

where m is an integer.

There is no analytical solution for maxima, so we must use a geometrical method to obtain them. Cancellation of the cosine term in Eq. (24),

$$\cos\left\{\frac{kn_0}{4} \frac{h^2 g_0}{\tan[g_0(z' - z)]}\right\} = 0, \quad (27)$$

yields the points

$$\bar{z}' = \frac{1}{g_0} \tan^{-1}\left[\frac{n_0 h^2 g_0}{(2m + 1)\lambda}\right] + z, \quad (28)$$

which are the maxima of the sine in Eq. (18) but not the maxima of irradiance.

We now represent the left-hand side of Eq. (24) as a function of z' and also, separately, the first and second terms of the same equation (see Fig. 4). We can estimate the maxima positions by paying attention to the area around positions \bar{z}' (or, equivalently, positions A), which is shown as an enlargement in Fig. 4(b). Knowing position A, one can easily determine position B, so that the length of segment \overline{AB} is

$$\overline{AB} = \cos^{-1}\left\{\tan^{-1}\left[\frac{n_0 h^2 g_0}{(2m + 1)\lambda}\right]\right\}. \quad (29)$$

Keeping in mind that $\overline{AB} \equiv \overline{CD}$, we can calculate the displacement AC by means of the tangent of angle α , which is the derivative of the second term in Eq. (24):

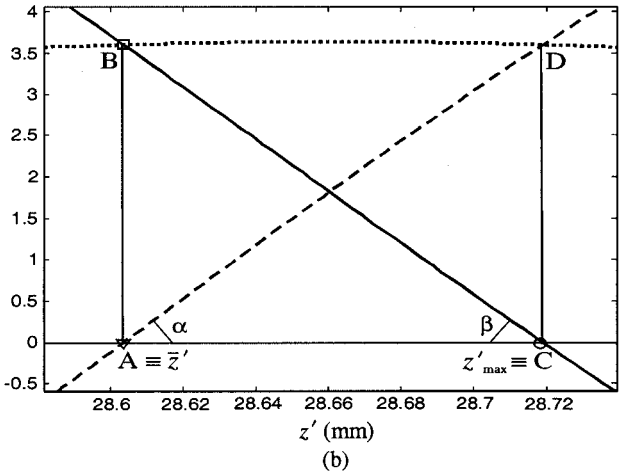
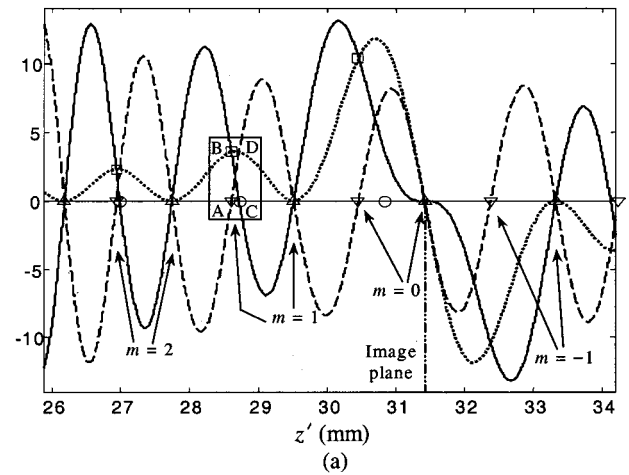


Fig. 4. Geometrical method for estimation of the positions of the maxima of irradiance when the wave front is located at a Fourier transform plane. (a) Shown are the left-hand side of Eq. (24) (solid curve) and the first (dashed curve) and second (dotted curve) terms of that equation. Squares, intersections of the solid and dashed curves (positions B); triangles, positions of the minima of irradiance; inverted triangles, positions \bar{z}' ; circles, calculated positions of the maxima of irradiance. We observe that for $m = 0$ our calculation is wrong: the principal maximum is at the image plane in variable z . (b) Enlargement of the area selected by a box in (a).

$$\tan \alpha \equiv \tan \beta = \frac{k^2 n_0^2}{16} h^4 g_0^3 \sin^{-5}\left\{\tan^{-1}\left[\frac{n_0 h^2 g_0}{(2m + 1)\lambda}\right]\right\}. \quad (30)$$

The length of segment \overline{AC} is then

$$\overline{AC} = \frac{\overline{CD}}{\tan \alpha}$$

$$= \frac{4\lambda}{\pi^2 n_0 h^2 g_0^2 (2m + 1)} \sin^4\left\{\tan^{-1}\left[\frac{n_0 h^2 g_0}{(2m + 1)\lambda}\right]\right\}, \quad (31)$$

and we conclude that the maxima are at positions

$$z'_{\max} \equiv C = \bar{z}' + \overline{AC} \cong z + \frac{1}{g_0} \tan^{-1} \left[\frac{n_0 h^2 g_0}{(2m+1)\lambda} \right] + \frac{4\lambda}{\pi^2 n_0 h^2 g_0^2 (2m+1)} \sin^4 \left\{ \tan^{-1} \left[\frac{n_0 h^2 g_0}{(2m+1)\lambda} \right] \right\}. \quad (32)$$

This is only an approximated value; the approximation is more accurate for higher orders of m . Note that in a homogeneous medium, $g_0 = 0$ and $\overline{AC} \rightarrow 0$.

The principal maximum is located at positions given by $m = 0$ only when

$$\left| \tan^{-1} \left(\frac{n_0 h^2 g_0}{2\lambda} \right) - \frac{\pi}{2} \right| > \pi, \quad (33)$$

which is fulfilled for small g_0 and h , and large λ . This condition comes from a comparison of the behavior of the sine and $H_2(z')$ terms in Eq. (18) for different values of g_0 , λ , and h ; the greater the first member of Eq. (33) is than π , the better the condition is verified. In this case, the width of the first peak of the sine is greater than the width of the cosine and the irradiance has a principal maximum where Eq. (32) predicts it. When the first member of Eq. (33) is much smaller than π , the width of the cosine is much greater than the width of the sine and the principal maximum is always located at $z'_{\max} = \pi/g_0$ (Fourier transform plane in variable z' or image plane of the point source). The irradiance at its peak is given by

$$I(z'_{\max} = \pi/g_0) = \frac{k^4 n_0^4 g_0^4}{16\pi^2} h^4. \quad (34)$$

In Fig. 4, parameters were chosen in order to be in this case, and thus the principal maximum is at the image planes in variable z . In Fig. 5 the irradiance is represented along the z' axis.

Up to this point we have dealt with the two extreme cases. If we make the first term of Eq. (33) be approximately π , the principal maximum is not at the image

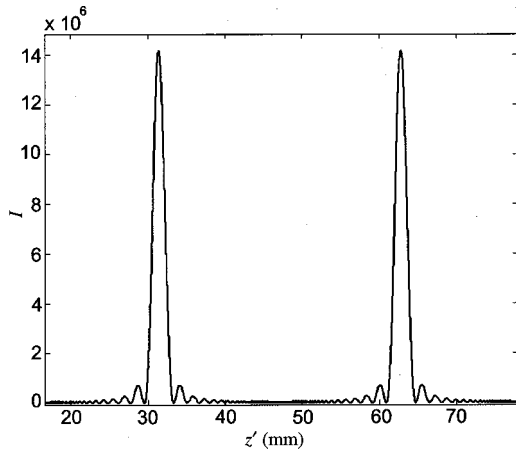


Fig. 5. Variation of the irradiance with the position inside the GRIN medium when the wave front is at a Fourier transform plane. Calculations were made for $n_0 = 1.5$, $g_0 = 0.1 \text{ mm}^{-1}$, and $h = 0.3 \text{ mm}$. Maxima are at image planes in variable z .

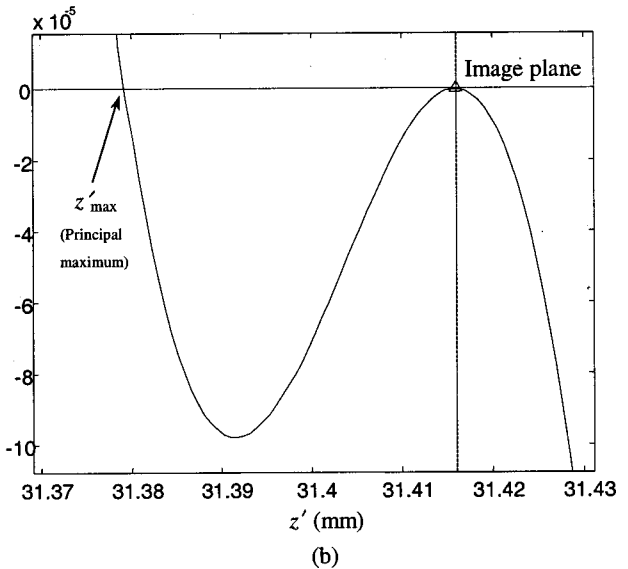
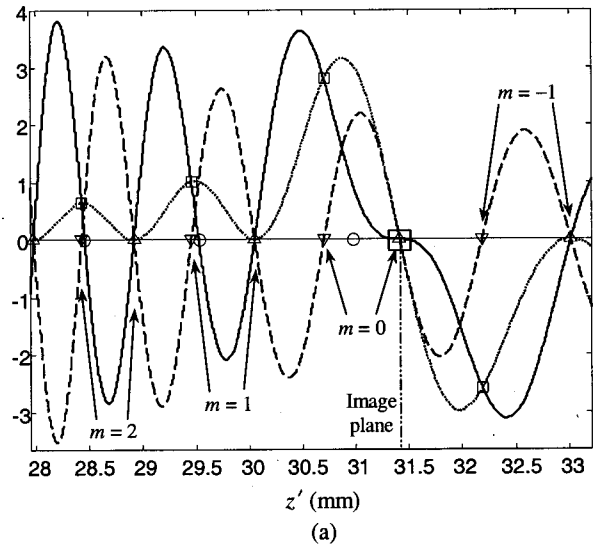


Fig. 6. Estimation of the positions of the maxima of irradiance when the wave front is off a Fourier transform plane. (b) Enlargement of the area around the image plane.

plane, but neither can it be predicted by Eq. (32). It tends to this predicted value as the first term in Eq. (33) increases.

B. Wave Front off Fourier Transform Planes

Figure 6 is the equivalent of Fig. 4 for a wave front off the Fourier planes. We can apply a geometrical method similar to the one used in the previous case to calculate the positions of the maxima of irradiance.

Proceeding as in Subsection 4.A, we obtain for the irradiance distribution in Eq. (12) that the minima are at

$$z'_{\min} = \frac{1}{g_0} \tan^{-1} \left\{ g_0 / \left[\frac{2m\lambda}{n_0 h^2} - \frac{\dot{H}_1(z)}{H_1(z)} \right] \right\} + z. \quad (35)$$

Likewise, positions \bar{z}' are given by

$$z' = \frac{1}{g_0} \tan^{-1} \left\{ g_0 \left/ \left[\frac{(2m+1)\lambda}{n_0 h^2} - \frac{\dot{H}_1(z)}{H_1(z)} \right] \right. \right\} + z. \quad (36)$$

Consequently, the maxima are located at

$$z'_{\max} \equiv C = \bar{z}' + \overline{AC} \equiv z + \frac{1}{g_0} \tan^{-1} \left\{ g_0 \left/ \left[\frac{(2m+1)\lambda}{n_0 h^2} - \frac{\dot{H}_1(z)}{H_1(z)} \right] \right. \right\} + \frac{[H_1(z)g_0 \sin(g_0 z'_{\max} - z) + \dot{H}_1(z) \cos(g_0 z'_{\max} - z)] \sin^4(g_0 z'_{\max} - z)}{\frac{k^2 n_0^2}{16} h^4 g_0^4 \left[\frac{\dot{H}_1(z)}{g_0} \sin(g_0 z'_{\max} - z) + H_1(z) \cos(g_0 z'_{\max} - z) \right]}. \quad (37)$$

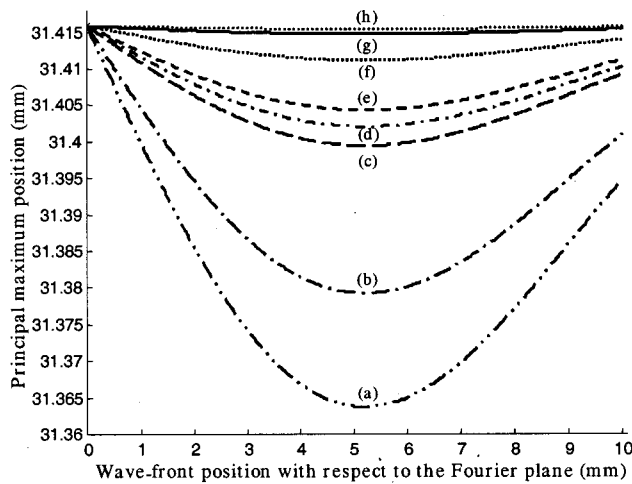


Fig. 7. Principal maximum position as a function of the displacement of the wave front from the Fourier transform planes for curves (a) $h = 0.3$ mm and $\lambda = 1.55$ μm , (b) $h = 0.3$ mm and $\lambda = 1.3$ μm , (c) $h = 0.4$ mm and $\lambda = 1.3$ μm , (d) $h = 0.3$ mm and $\lambda = 0.8$ μm , (e) $h = 0.4$ mm and $\lambda = 1.3$ μm , (f) $h = 0.5$ mm and $\lambda = 1.3$ μm , (g) $h = 0.7$ mm and $\lambda = 1.3$ μm , and (h) $h = 0.7$ mm and $\lambda = 0.8$ μm . We took $g_0 = 0.1$ mm^{-1} and the first image plane to be at $z' = 10\pi$ mm.

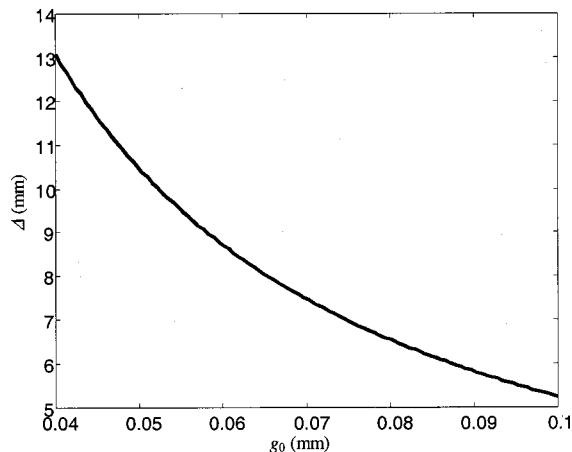


Fig. 8. Wave-front position with respect to the Fourier plane for which the turning point of the principal maximum is achieved (Δ) as a function of the gradient parameter g_0 .

As in Subsection 4.A, $m = 0$ provides the principal maximum position only when the condition in Eq. (33) is verified. Figure 6 shows the case in which the first term of Eq. (33) is much greater than π . We can observe that the principal maximum is no longer at image planes in z vari-

able [it is slightly shifted from those planes, as shown in the enlargement in Fig. 6(b)] as happened when the wave front was at the Fourier transform planes. In Fig. 7 we show the principal maximum position as a function of the wave-front position measured from the Fourier plane. We observe that the variation in the principal maximum position decreases with increasing h and decreasing λ . On the other hand, as the wave front shifts from the Fourier transform planes, the principal maximum moves away from the image planes and subsequently approaches them again. The maximum shift from the image planes is, however, achieved for the same wave-front location in all cases, which leads us to conclude that the maximum shift is only a function of the medium characteristics. In particular, that turning point of the principal maximum varies inversely as the gradient parameter g_0 (Fig. 8).

5. ZONE CONTRIBUTION TO THE TOTAL DISTURBANCE

Equation (8) allowed us to determine the total disturbance at a point z' that is due to a circular aperture of radius h . To find the contribution of a single zone, we only have to change the limits of integration and choose them to go from h_{j-1} to h_j . Hence, for wave fronts at Fourier transform planes and off them, the contribution of the j th zone to the field at z' is given, respectively, by

$$\psi_j(z') = (-1)^{j-1} \frac{2i \zeta(z, z')}{B(z, z')}, \quad (38)$$

$$\psi_j(z') = (-1)^{j-1} \frac{2i \zeta(z, z')}{B(z, z')} \times \left[1 - \frac{\dot{H}_1^2(z)}{2B(z, z')H_1^2(z)} (\pi - j2\pi - 2i) \right]. \quad (39)$$

We note that the contributions of the successive zones are alternately positive and negative. The total effect at z' is obtained by summing all these contributions. If j is even,

a minimum is obtained at z' , and if j is odd, the irradiance will give a maximum:

$$I(z') = \left| \sum_j \psi_j(z') \right|^2 = \begin{cases} \frac{4|\zeta(z, z')|^2}{B^2(z, z')} & \text{if } j \text{ is odd} \\ 0 & \text{if } j \text{ is even} \end{cases}, \quad (40)$$

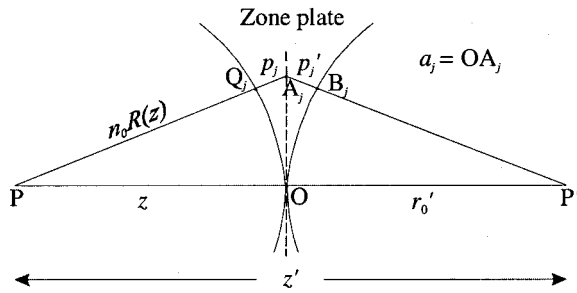


Fig. 9. Geometry for calculation of the ring radii of a zone plate in a GRIN medium.

$$I(z') = \left| \sum_j \psi_j(z') \right|^2 = \begin{cases} \frac{4|\zeta(z, z')|^2}{B^2(z, z')} \left[1 + \frac{H_1^2(z)}{B(z, z')H_1^2(z)} j\pi \right] & \text{if } j \text{ is odd} \\ 0 & \text{if } j \text{ is even.} \end{cases} \quad (41)$$

Equation (40) is the irradiance for wave fronts at Fourier transform planes, and Eq. (41) is for wave fronts off Fourier transform planes. In both we have disregarded the terms that go with $H_1^4(z)/H_1^4(z)$. Seeing these equations, we conclude that for wave fronts at Fourier transform planes all the zones contribute in the same way, whereas the contributions are slightly different for wave fronts shifted from those planes because of the dependence of the irradiance on j .

6. ZONE-PLATE CONSTRUCTION

To calculate the ring radii of a planar zone plate for a paraboloidal wave front [Eq. (2)] in a GRIN medium, let us take into account Fig. 9. From triangles PA_jP' and

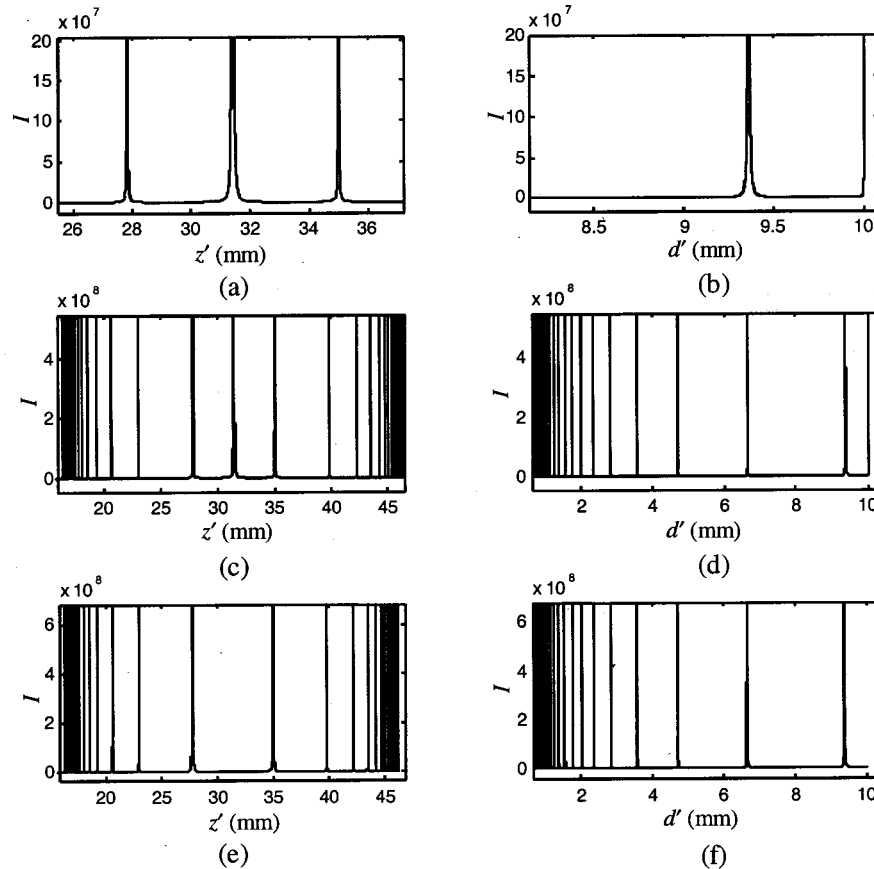


Fig. 10. Irradiance in terms of the optical axis z' [(a), (c), and (e)] and the equivalent object distance d' [(b), (d), and (f)] when a sinusoidal zone plate of the amplitude, a Fresnel zone plate of the amplitude, and a Fresnel zone plate of the phase, respectively, are placed at a Fourier transform plane in a selfoc medium. Calculations were made for $\lambda = 1.3 \mu\text{m}$, $n_0 = 1.5$, $g_0 = 0.1 \text{ mm}^{-1}$, $z'_r = 35 \text{ mm}$, and position of the wave front $z = 5\pi \text{ mm}$.

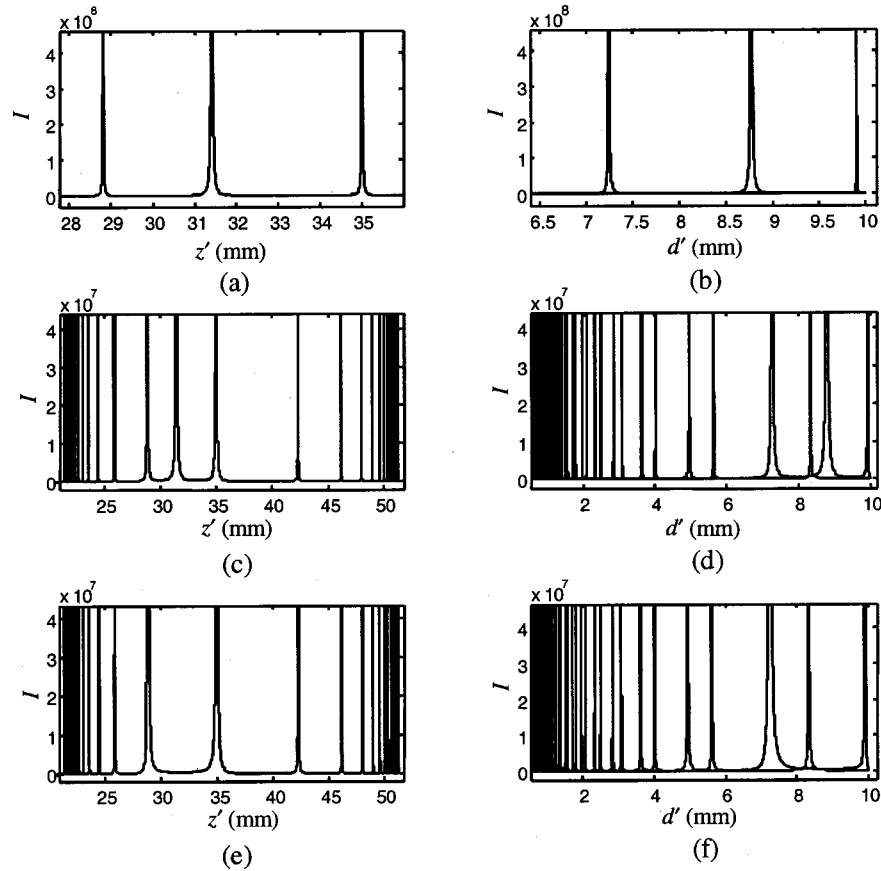


Fig. 11. Irradiance in terms of the optical axis z' [(a), (c), and (e)] and the equivalent object distance d' [(b), (d), and (f)] when a sinusoidal zone plate of the amplitude, a Fresnel zone plate of the amplitude, and a Fresnel zone plate of the phase, respectively, are placed off a Fourier transform plane in a selfoc medium. Calculations were made for $\lambda = 1.3 \mu\text{m}$, $n_0 = 1.5$, $g_0 = 0.1 \text{ mm}^{-1}$, $z'_r = 35 \text{ mm}$, and position of the wave front $z = 20.708 \text{ mm}$.

$P'A_jO$ we obtain

$$a_j^2 = (n_0R(z) + p_j)^2 - z^2 = (r_0' + p_j')^2 - r_0'^2. \quad (42)$$

As $n_0R(z) \sim z$, and $z \gg p_j$ and $r_0' \gg p_j'$, since slow variations of z within a zone have been considered, we can disregard the squares of p_j and p_j' and write

$$a_j^2 \cong 2n_0R(z)p_j \cong 2r_0'p_j'. \quad (43)$$

From here it follows that

$$p_j \cong \frac{a_j^2}{2n_0R(z)}, \quad p_j' \cong \frac{a_j^2}{2r_0'}. \quad (44)$$

But the light that is propagated along PA_jP' travels a path that is longer by the amount

$$\frac{j\lambda H_1(z')R(z)}{2(z' - z)[n_0H_2(z')R(z) + H_1(z')]} + \frac{j\lambda H_1(z')}{2n_0[H_1(z') + n_0R(z)H_2(z')]} \quad (45)$$

than the one that follows POP' , where Eqs. (15) and (16) have been used. Then we can write

$P'A_jP - P'OP$

$$\begin{aligned} &= n_0R(z) + p_j + p_j' + r_0' - (z + r_0') \\ &= p_j + p_j' \\ &= \frac{j\lambda H_1(z)H_1(z')}{2(z' - z)n_0[\dot{H}_1(z)H_1(z') + H_2(z')H_1(z)]} \\ &\quad + \frac{j\lambda \dot{H}_1(z)H_1(z')}{2n_0[\dot{H}_1(z)H_1(z') + H_1(z)H_2(z')]} \end{aligned} \quad (46)$$

and, relations (44), we can express Eq. (46) as

$$\frac{a_j^2}{2} \left[\frac{1}{n_0R(z)} + \frac{1}{r_0'} \right] = \frac{j\lambda H_1(z)H_1(z')}{2n_0[\dot{H}_1(z)H_1(z') + H_2(z')H_1(z)]} \times \left[\frac{1}{(z' - z)} + \frac{\dot{H}_1(z)}{H_1(z)} \right]. \quad (47)$$

Now considering $r_0' = z' - z$, we obtain

$$a_j^2 = \frac{j\lambda H_1(z)H_1(z')}{n_0[\dot{H}_1(z)H_1(z') + H_2(z')H_1(z)]} \equiv h_j^2, \quad (48)$$

which coincides with Eq. (14). Therefore the planar zone-plate ring radii coincide, in first approximation, with the zone radii of the paraboloidal wave front.

Equation (48) can be regarded as the formula of an apparent lens,

$$\frac{\dot{H}_1(z)}{H_1(z)H_2(z')} + \frac{1}{H_1(z')} = \frac{j\lambda}{n_0h_j^2H_2(z')} \quad (49)$$

$$\Leftrightarrow \frac{1}{f} = \frac{1}{d} + \frac{1}{d'},$$

where

$$f = \frac{n_0h_j^2H_2(z')}{j\lambda} = \frac{n_0h_1^2H_2(z')}{\lambda} \quad (50)$$

is the focal length,

$$d = \frac{H_1(z)H_2(z')}{\dot{H}_1(z)} = n_0R(z)H_2(z') \quad (51)$$

is the object distance, and

$$d' = H_1(z') \quad (52)$$

is the image distance. The focal length f is defined as the distance d' where light is focused when the zone plate is

located on a plane such that the curvature radius $R(z)$ tends to infinity, that is, at a Fourier transform plane.

There are different kinds of tapered GRIN media depending on the functional form of $g(z)$. Let us apply the zone-plate construction to the well-known selfoc media and to media with divergent linear and parabolical taper functions (whose importance as focusers and collimators in optical communications must be emphasized) given, respectively, by

$$g(z) = \frac{g_0}{1+z/L}, \quad g(z) = \frac{g_0}{(1+z/L)^2}, \quad (53)$$

where L is the distance from $z = 0$ to the common apex of the equi-index lines, and $g_0 = g(0)$. The axial and the field rays for these media are, respectively,

$$H_{1l}(z) = \frac{(L+z)^{1/2}}{L^{1/2}g_0} \sin \left[g_0L \ln \left(1 + \frac{z}{L} \right) \right],$$

$$H_{1l}(z') = \frac{(L+z')^{1/2}}{L^{1/2}g_0} \sin \left[g_0L \ln \left(\frac{L+z'}{L+z} \right) \right]; \quad (54)$$

$$H_{2l}(z) = \left(\frac{L+z}{L} \right)^{1/2} \cos \left[g_0L \ln \left(1 + \frac{z}{L} \right) \right],$$

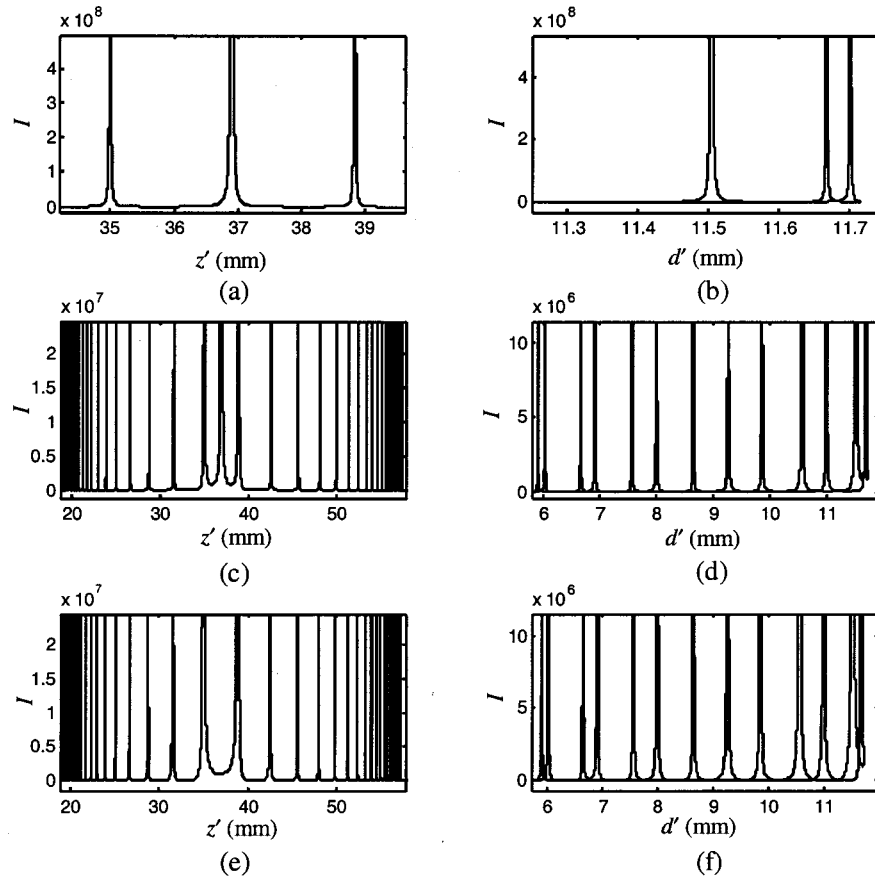


Fig. 12. Irradiance in terms of the optical axis z' [(a), (c), and (e)] and the equivalent object distance d' [(b), (d), and (f)] when a sinusoidal zone plate of the amplitude, a Fresnel zone plate of the amplitude, and a Fresnel zone plate of the phase, respectively, are placed at a Fourier transform plane in a linear divergent medium. Calculations were made for $\lambda = 1.3 \mu\text{m}$, $n_0 = 1.5$, $g_0 = 0.1 \text{ mm}^{-1}$, $L = 100 \text{ mm}$, $z'_r = 35 \text{ mm}$, and position of the wave front $z = 17.009 \text{ mm}$.

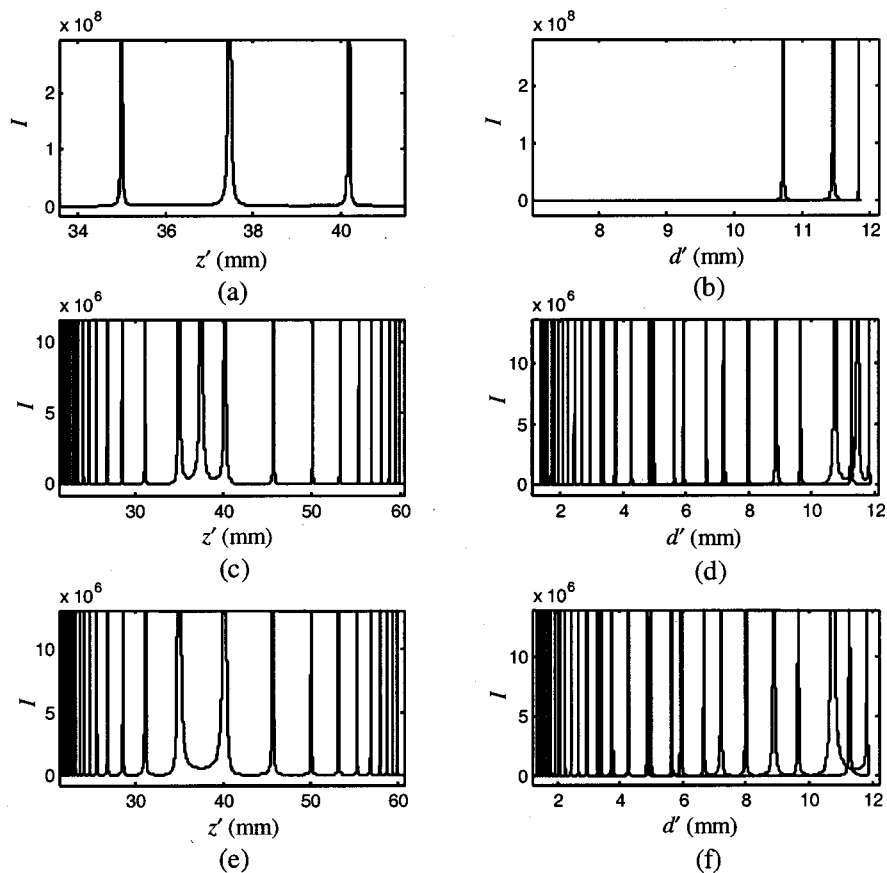


Fig. 13. Irradiance in terms of the optical axis z' [(a), (c), and (e)] and the equivalent object distance d' [(b), (d), and (f)] when a sinusoidal zone plate of the amplitude, a Fresnel zone plate of the amplitude, and a Fresnel zone plate of the phase, respectively, are placed off a Fourier transform plane in a linear divergent medium. Calculations were made for $\lambda = 1.3 \mu\text{m}$, $n_0 = 1.5$, $g_0 = 0.1 \text{mm}^{-1}$, $L = 100 \text{mm}$, $z'_r = 35 \text{mm}$, and position of the wave front $z = 20.009 \text{mm}$.

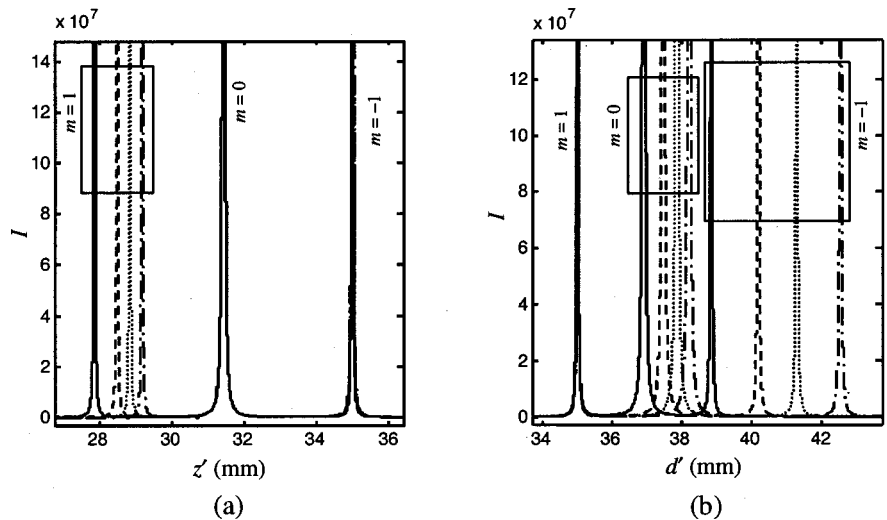


Fig. 14. Diffractive-order shifts when the wave-front position moves from the Fourier transform planes for (a) a selfoc medium and (b) a linear divergent medium. Solid curve, wave front at the Fourier transform plane, dashed, dotted, and dashed-dotted curves, wave fronts displaced 3, 5, and 7 mm from the Fourier transform plane, respectively.

$$H_{2l}(z') = \left(\frac{L+z'}{L}\right)^{1/2} \cos\left[g_0 L \ln\left(\frac{L+z'}{L+z}\right)\right]; \quad (55)$$

and

$$H_{1p}(z) = \frac{L+z}{Lg_0} \sin\left[\frac{g_0 L z}{L+z}\right],$$

$$H_{1p}(z') = \frac{L+z'}{Lg_0} \sin\left[g_0 L^2 \left(\frac{1}{L+z} - \frac{1}{L+z'}\right)\right]; \quad (56)$$

$$H_{2p}(z) = \frac{L+z}{L} \cos\left[\frac{g_0 L z}{L+z}\right],$$

$$H_{2p}(z') = \frac{L+z'}{L} \cos\left[g_0 L^2 \left(\frac{1}{L+z} - \frac{1}{L+z'}\right)\right]. \quad (57)$$

Substitution of Eqs. (22), (23), and (54)–(57) into Eqs. (50), (51), and (52) produces

$$f_{\text{sf}} = \frac{\sin(g_0 z) \sin[g_0(z_r' - z)] \cos[g_0(z' - z)]}{g_0 \{ \cos(g_0 z) \sin[g_0(z_r' - z)] + \sin(g_0 z) \cos[g_0(z_r' - z)] \}}, \quad (58)$$

$$d_{\text{sf}} = \frac{1}{g_0} \tan(g_0 z) \cos[g_0(z' - z)], \quad (59)$$

$$d_{\text{sf}}' = \frac{1}{g_0} \sin[g_0(z' - z)], \quad (60)$$

for a selfoc medium;

$$f_l = \frac{(L+z)(L+z')^{1/2} \sin\left[g_0 L \ln\left(1 + \frac{z}{L}\right)\right] \sin\left[g_0 L \ln\left(\frac{L+z_r'}{L+z}\right)\right] \cos\left[g_0 L \ln\left(\frac{L+z'}{L+z}\right)\right]}{g_0 \left\{ L^{3/2} \cos\left[g_0 L \ln\left(1 + \frac{z}{L}\right)\right] \sin\left[g_0 L \ln\left(\frac{L+z_r'}{L+z}\right)\right] + (L+z)L^{1/2} \sin\left[g_0 L \ln\left(1 + \frac{z}{L}\right)\right] \cos\left[g_0 L \ln\left(\frac{L+z_r'}{L+z}\right)\right] \right\}}, \quad (61)$$

$$d_l = \frac{(L+z)(L+z')^{1/2}}{L^{3/2} g_0} \tan\left[g_0 L \ln\left(1 + \frac{z}{L}\right)\right], \quad (62)$$

$$d_l' = \left(\frac{L+z'}{Lg_0^2}\right)^{1/2} \sin\left[g_0 L \ln\left(\frac{L+z'}{L+z}\right)\right], \quad (63)$$

for a divergent linear medium; and

$$f_p = \frac{(L+z)^2(L+z') \sin\left(\frac{g_0 L z}{L+z}\right) \sin\left[g_0 L^2 \left(\frac{1}{L+z} - \frac{1}{L+z_r'}\right)\right] \cos\left[g_0 L^2 \left(\frac{1}{L+z} - \frac{1}{L+z'}\right)\right]}{g_0 \left\{ L^3 \cos\left(\frac{g_0 L z}{L+z}\right) \sin\left[g_0 L^2 \left(\frac{1}{L+z} - \frac{1}{L+z_r'}\right)\right] + L(L+z)^2 \sin\left(\frac{g_0 L z}{L+z}\right) \cos\left[g_0 L^2 \left(\frac{1}{L+z} - \frac{1}{L+z_r'}\right)\right] \right\}} \quad (64)$$

$$d_p = \frac{(L+z)^2(L+z')}{L^3 g_0} \tan\left(\frac{g_0 L z}{L+z}\right) \cos\left[g_0 L^2 \left(\frac{1}{L+z} - \frac{1}{L+z'}\right)\right] \quad (65)$$

$$d_p' = \frac{L+z'}{Lg_0} \sin\left[g_0 L^2 \left(\frac{1}{L+z} - \frac{1}{L+z'}\right)\right], \quad (66)$$

for a divergent parabolical medium. Variable z_r' represents the position z' for which radius h_1 is calculated.

Figures 10 and 11 show the variation of the irradiance along the optical axis in a selfoc medium for a wave front placed at the Fourier transform plane and off it, respectively, and for three types of zone-plate transmission functions, namely, a sinusoidal zone plate of the amplitude and a Fresnel zone plate of the amplitude and of the phase. We can observe that there are several peaks of irradiance, each of which corresponds to a diffractive order. The positive and negative orders are placed symmetrically with respect to order zero in Fig. 10, but the symmetry is lost in Fig. 11.

Figures 12 and 13 are equivalent to Figs. 10 and 11 but for a linear divergent medium. In this medium we cannot observe any symmetry between the diffractive orders. Figure 14 shows the irradiance for various positions of the wave front in a (a) selfoc medium and (b) a linear divergent medium when a sinusoidal zone plate of the ampli-

tude is placed in front of the wave front. We can observe the shift of the diffractive orders as the wave front moves from the Fourier transform plane. Note that in a selfoc medium, the order zero does not change its position, whereas it changes for a linear divergent medium.

Finally, for free space, where $g(z) \rightarrow 0$; $n_0 = 1$; $H_1(z) \rightarrow z$, $H_1(z') \rightarrow z' - z$; and $H_1(z)$, $H_2(z') \rightarrow 1$, the object and image distances become, respectively, $d = z$ and $d' = z' - z$, which coincide with the classic results.⁶

7. CONCLUSIONS

A wave front that propagates in a GRIN medium was divided into periodic zones by calculating the difference in optical path between successive zones. We determined the radii and the areas of those zones, finding that they coincide for each zone when the wave front is situated at a Fourier transform plane. Once this was done, we obtained the disturbance produced by these zones separately at a point on the optical axis, noticing that the contributions of the zones were alternately positive and negative. The fact that successive zones provoke contributions to the total disturbance that tend to cancel each other out implies that we would observe a huge increase in the irradiance at a point if we eliminated all the even

or odd zones. This suggests and justifies the construction of zone plates in GRIN media, which was discussed in Section 6.

ACKNOWLEDGMENTS

This work was supported by the Ministerio de Ciencia y Tecnología, Spain, under contract TIC99-0489.

REFERENCES

1. J. Ojeda-Castañeda and C. Gómez-Reino, eds., *Selected Papers on Zone Plates*, Vol. MS 128 of SPIE Milestone Series (SPIE Press, Bellingham, Wash., 1996), and references therein.
2. J. M. Rivas-Moscoso, C. Gómez-Reino, C. Bao, and M. V. Pérez, "Tapered gradient-index media and zone plates," *J. Mod. Opt.* **47**, 1549–1567 (2000).
3. J. M. Rivas-Moscoso, C. Gómez-Reino, M. V. Pérez, and C. Bao, "Tapered gradient-index and zone plates: influence of off-axis illumination and finite dimension on light propagation," *J. Mod. Opt.* **48**, 915–926 (2001).
4. Yu. A. Kravtsov and Yu. I. Orlov, *Geometrical Optics of Inhomogeneous Media* (Springer-Verlag, Berlin, 1990), Sec. 2.10.2.
5. C. Gómez-Reino, M. V. Pérez, and C. Bao, *GRIN Optics: Fundamentals and Applications* (Springer, Berlin, 2002), Chaps. 1 and 2.
6. M. Born and E. Wolf, *Principles of Optics* (Cambridge U. Press, Cambridge, UK, 1997), Chap. VIII.